ISSN 1392 - 1207. MECHANIKA. 2012 Volume 18(1): 5-13

Comprehensive thermoelastic analysis of a functionally graded cylinder with different boundary conditions under internal pressure using first order shear deformation theory

M. Arefi*, G.H. Rahimi**
**Tarbiat Modares University, Tehran, Iran, 14115-143, E-mail: arefi63@gmail.com*
***Tarbiat Modares University, Tehran, Iran, 14115-143, Corresponding author: E-mail: rahimi_gh@modares.ac.ir*
crossref http://dx.doi.org/10.5755/j01.mech.18.1.1273

1. Introduction

With advancing the techniques of material production, new group of materials which are called functionally graded materials (FGMs) are appeared in industrial applications. The first idea for producing this group of materials was their application in high temperature gradient environment and their forming ability. For the structures that are applicable in the environments such as nuclear reactors and chemical laboratories, it is inevitable to use FGMs. FGMs are made of a mixture with arbitrary composition of two different materials, and volume fraction of each material changes continuously and gradually at the entire volume of the material. Ceramic and metal are the examples of these different materials. Ceramics bear high gradient temperature and keep the first configuration. If we use the pure metal in those environments, in the effect of high temperature, creep and large deformation in structure was inevitable.

Ceramics have a high resistance to forming in temperature field and in other hand metals have a ductility property that diminishes fragility of ceramics. As mentioned above, compounding of ceramic and metal can be used to create the best property for bearing the entire unwanted environment [1].

One of the most applicable structures in the mechanical engineering is the shells. In the general state, they can be classified to two classes. First class of them is thin. This class is applicable for bearing the membrane and in-plane forces. Membrane theory can be used to utilize this class of shell. Second classes of shells are the thick shells. In this class, total deformation of shell includes displacement of middle surface and rotation about middle surface of the shell. Thick shells can be applied to undergo bending and stretching force, simultaneously.

Lame studied the exact solution of a thick walled cylinder under inner and outer pressure. The cylinder is supposed to be axisymmetric and isotropic [2]. Naghdi [3] considered the effect of lateral shear and consequently, constitute the theory of shear deformation. Mirsky and Hermann [4] applied the first order shear deformation theory (FSDT) for the analysis of an isotropic cylinder. FGMs are created by one Japanese group of material scientist [5]. Properties of this group of materials are varying continuously at the entire volume of the material.

At the first years of decade 1990, researches on the thermal and vibration analysis of FGM were started. Tutuncu and Ozturk [6] presented the exact solution of a FG spherical and cylindrical pressure vessel. Jabbari et al [7] analyzed the thermoelastic analysis of a FG cylinder under the thermal and mechanical loads. It has been supposed that the material properties are varying as a power function in terms of the radial coordinate system. With substitution of the derived temperature field in the navier equation, the obtained differential equation has been solved analytically.

Wu et al [8] investigated the elastic stability of a FG cylinder. They employed the shell Donnell's theory to derive the strain-deformation relations. Stress-strain equation has been obtained by consideration the effect of thermal strain in Hooke's low. Three nonlinear equations of equilibrium according to Donnell's theory have been applied. Imposing the condition of prebuckling and a function for the radial displacement, the results have been defined by minimization of the critical load with respect to defined parameter of the problem. The buckling load of cylinder has been evaluated under uniform temperature rising. Shao [9] investigated the thermo elastic analysis of a thick walled cylinder under the mechanical and thermal loads. The cylinder has been divided into many annular sub cylinders in the radial direction. Based on this division, properties of every sub cylinder may be assumed to be uniform. In the following, it is employed the thermal and the equilibrium equation for every subcylinder, individually. After solution of the thermal and the equilibrium equation in every subcylinder, compatibility equations for the thermal and mechanical components within the every two layers are imposed. By doing this procedure for the complete cylinder, distribution of temperature and displacement have been obtained.

Eslami et al [10] studied a general solution for the one-dimensional steady-state thermal and mechanical stresses in a hollow thick sphere made of functionally graded material. The temperature distribution is assumed to be a function of radius, with general thermal and mechanical boundary conditions on the inside and outside surfaces of the sphere. The material properties, except Poisson’s ratio, are assumed to vary along the radius according to a power law function. The navier equation is solved analytically with evaluation of the roots of the characteristic equation.

The coupled thermoelastic response of a functionally graded circular cylindrical shell is presented by Bahtui et al [11]. The coupled thermoelastic and the energy equations are simultaneously solved for a functionally graded axisymmetric cylindrical shell. A second-order shear deformation shell theory is considered for that analysis. The shell is graded through the thickness assuming a volume fraction of metal and ceramic, using a power law distribution. Khabbaz et al [12] employed the first and third order shear deformation theories to predict the large deflection of FG plates. The results indicated that the energy method powered by the FSDT and FSDT is capable of predicting the behavior of a FG structure such as plate. Jabbari et al [13] investigated the thermo elastic behavior of a FG cylinder under the thermal and the mechanical loads. Firstly, they employed two-dimensional differential equation of heat transfer for the different boundary conditions. By considering two equations of equilibrium in the cylindrical coordinate system and imposing the distribution of temperature, they obtained two navier equations in terms of two axisymmetric components of displacement.

As a main applicable instance of shells, cylindrical shell can be considered in the present paper. Pressure vessels, reactors, heat exchanger and other nuclear and chemical equipments are the instances of the cylindrical shells. Present study would improve the manufacturing of chemical and weapon equipments and then increases the strength of them by using the FGM. The present study considers the effect of the pressure and temperature on the behavior of a FG cylinder with different boundary conditions, simultaneously. The present paper proposes an analytical method for two dimensional analysis of a FG cylinder. This solution considers the end effect of cylinder. The previous papers have not been considered the end effect of cylinder actually and comprehensively [13].

2. Formulation

In the present study, the first order shear deformation Mirsky-Herman theory is employed to simulate deformation of every layer of the cylinder in terms of displacement of midsurface and rotation about outward axis of the middle surface [4]. Before demonstration of the procedure of FSDT, it is necessary to expand Lame's solution for a cylindrical pressure vessel. In the Lame's theory, symmetrical distribution of the radial displacement, *u* may be obtained as follows [4, 14]

$$u = c_1 r + \frac{c_2}{r} \tag{1}$$

where *r* is the radius of every layer of the cylinder. In the general state, this distance can be obtained in terms of the radius of the midsurface *R* and distance of every layer with respect to midsurface ρ as follows

$$r = R + \rho \tag{2}$$

By substitution of *r* into the Lame's solution (Eq. (1)) and applying the Taylor expansion, Eq. (1) may be obtained as a function of ρ as follows

$$u = c_1(R+\rho) + \frac{c_2}{R+\rho} = c_0' + c_1'\rho + \ldots \tag{3}$$

Eq. (3) has been known as the first order shear deformation theory (FSDT). Based on this theory, every component of the deformation states by two variables including the rotation and displacement. For a symmetric cylindrical shell, the radial and axial components of deformation may be considered as follows [15-17]

$$\begin{Bmatrix} u_z \\ w_r \end{Bmatrix} = \begin{Bmatrix} u \\ w \end{Bmatrix} + \rho \begin{Bmatrix} \phi_z \\ \phi_r \end{Bmatrix} \tag{4}$$

where u_z, w_z are the axial and radial components of displacement, respectively. u, w, ϕ_x, ϕ_z are the functions of axial component of coordinate system (z) only. With consideration of the Eq. (4) and recalling $\frac{\partial}{\partial r} = \frac{\partial}{\partial z}$ from Eq. (2), the components of strains ε_i are [15-17]

$$\begin{cases} \varepsilon_z = \dfrac{\partial u_z}{\partial z} = \dfrac{\partial u}{\partial z} + \rho \dfrac{\partial \phi_z}{\partial z} \\ \varepsilon_r = \dfrac{\partial w_r}{\partial \rho} = \phi_r \\ \varepsilon_\theta = \dfrac{w_r}{r} = \dfrac{w + \rho\phi_r}{R+\rho} \\ \gamma_{rz} = 2\times\varepsilon_{rz} = \dfrac{\partial u_z}{\partial \rho} + \dfrac{\partial w_r}{\partial z} = \phi_z + \dfrac{\partial w}{\partial z} + \rho\dfrac{\partial \phi_r}{\partial z} \end{cases} \tag{5}$$

Stress strain relations (Hooke's low) by consideration of the effect of the thermal strain are

$$\begin{cases} \varepsilon_z = \dfrac{\sigma_z - v(\sigma_r + \sigma_\theta)}{E} + \alpha T \\ \varepsilon_r = \dfrac{\sigma_r - v(\sigma_z + \sigma_\theta)}{E} + \alpha T \\ \varepsilon_\theta = \dfrac{\sigma_\theta - v(\sigma_r + \sigma_z)}{E} + \alpha T \\ \gamma_{rz} = 2\varepsilon_{rz} = \dfrac{\tau_{rz}}{G} \end{cases} \tag{6}$$

where σ_i are stress components and the material properties are considered according to reference [7]. By doing a little mathematical calculation, the components of stress in terms of strain components are

$$\begin{cases} \sigma_r = \dfrac{E}{(1+v)(1-2v)}\left\{(1-v)\varepsilon_r + v(\varepsilon_\theta + \varepsilon_z)\right\} - \dfrac{\alpha TE}{1-2v} \\ \sigma_\theta = \dfrac{E}{(1+v)(1-2v)}\left\{(1-v)\varepsilon_\theta + v(\varepsilon_r + \varepsilon_z)\right\} - \dfrac{\alpha TE}{1-2v} \\ \sigma_z = \dfrac{E}{(1+v)(1-2v)}\left\{(1-v)\varepsilon_z + v(\varepsilon_r + \varepsilon_\theta)\right\} - \dfrac{\alpha TE}{1-2v} \\ \tau_{rz} = \dfrac{E}{2(1+v)}\left\{\gamma_{rz}\right\} \end{cases} \tag{7}$$

Strain energy is equal to the one-half of multiplying of the components of stress tensor in the corresponding components of strain tensor. With having the components of the stresses and the strains, strain energy per unit volume $\bar{u}$ may be obtained as follows

$$\bar{u} = \frac{1}{2}\{\varepsilon\}^T\{\sigma\} = \frac{1}{2}\{\sigma_r\varepsilon_r + \sigma_z\varepsilon_z + \sigma_\theta\varepsilon_\theta + \tau_{rz}\gamma_{rz}\}\frac{1}{2}\frac{E}{(1+v)(1-2v)}\Big[(1-v)(\varepsilon_z{}^2 + \varepsilon_r{}^2 + \varepsilon_\theta{}^2) + 2v(\varepsilon_z\varepsilon_r + \varepsilon_z\varepsilon_\theta + \varepsilon_\theta\varepsilon_r) + \frac{1-2v}{2}\gamma_{rz}{}^2\Big] - \frac{\alpha TE}{2(1-2v)}(\varepsilon_z + \varepsilon_\theta + \varepsilon_r) \tag{8}$$

Eq. (8) includes two different expressions. The first class of them is the mechanical strain energy and the second class is the thermal strain energy. The total strain energy must be evaluated by integration of Eq. (8) on the volume of the cylinder. The volume element of the cylinder is $2\pi(R+\rho)d\rho dz$, therefore we'll have

$$dV = 2\pi(R+\rho)d\rho dz \rightarrow U = \iiint_V \bar{u} dV = \\ = \int_0^l [U_S(x) - U_T(x)]dz \tag{9}$$

where $U_S(\rho)$ is the mechanical strain energy and $U_T(\rho)$ is the thermal strain energy. With substitution of the strain component in terms of four displacement and rotation terms, mechanical and thermal energy (Eq. (9)) can be obtained by Eqs. (10)

$$\left. \begin{aligned} U_S &= \sum_{i=1}^{9} A_i(z) f_i(z) \rightarrow f_i(z) = f_i(u, w, \phi_z, \phi_r) \\ U_T &= \sum_{i=1}^{4} B_i(z) g_i(z) \rightarrow g_i(z) = g_i(u, w, \phi_z, \phi_r) \end{aligned} \right\} \tag{10}$$

where

$$A_1(z) = \int_{-\frac{h(z)}{2}}^{\frac{h(z)}{2}} \frac{\pi E(R+\rho)}{(1+v)(1-2v)} d\rho,\ f_1 = (1-v)\left[\phi_r^2 + \left(\frac{\partial u}{\partial z}\right)^2\right] + 2v\left[\phi_r \times \frac{\partial u}{\partial z}\right] + \frac{1-2v}{2}\left[\phi_z^2 + \left(\frac{\partial w}{\partial z}\right)^2 + 2\phi_z \frac{\partial w}{\partial z}\right],$$

$$A_2(z) = \int_{-\frac{h(z)}{2}}^{\frac{h(z)}{2}} \frac{\pi E\rho(R+\rho)}{(1+v)(1-2v)} d\rho,\ f_2 = (1-v)\left[2\frac{\partial u}{\partial z}\frac{\partial \phi_z}{\partial z}\right] + 2v\left[\phi_r \frac{\partial \phi_z}{\partial z}\right] + \frac{1-2v}{2}\left[2\phi_z \frac{\partial \phi_r}{\partial z} + 2\frac{\partial \phi_r}{\partial z}\frac{\partial w}{\partial z}\right],$$

$$A_3(z) = \int_{-\frac{h(z)}{2}}^{\frac{h(z)}{2}} \frac{\pi E\rho^2(R+\rho)}{(1+v)(1-2v)} d\rho,\ f_3 = (1-v)\left(\frac{\partial \phi_z}{\partial z}\right)^2 + \frac{1-2v}{2}\left(\frac{\partial \phi_r}{\partial z}\right)^2,\ A_4(z) = \int_{-\frac{h(z)}{2}}^{\frac{h(z)}{2}} \frac{\pi E}{(1+v)(1-2v)} d\rho,\ f_4 = 2v\left[w\phi_r + w\frac{\partial u}{\partial z}\right],$$

$$A_5(z) = \int_{-\frac{h(z)}{2}}^{\frac{h(z)}{2}} \frac{\pi E}{(R+\rho)(1+v)(1-2v)} d\rho,\ f_5 = (1-v)w^2,\ A_6(z) = \int_{-\frac{h(z)}{2}}^{\frac{h(z)}{2}} \frac{\pi E\rho}{(1+v)(1-2v)} d\rho,\ f_6 = 2v\left[\phi_r^2 + w\frac{\partial \phi_z}{\partial z} + \phi_r \frac{\partial u}{\partial z}\right]$$

$$A_7(z) = \int_{-\frac{h(z)}{2}}^{\frac{h(z)}{2}} \frac{\pi E\rho}{(R+\rho)(1+v)(1-2v)} d\rho,\ f_7 = (1-v)2\phi_r w,\ A_8(z) = \int_{-\frac{h(z)}{2}}^{\frac{h(z)}{2}} \frac{\pi E\rho^2}{(R+\rho)(1+v)(1-2v)} d\rho,\ f_8 = (1-v)\phi_r^2,$$

$$A_9(z) = \int_{-\frac{h(z)}{2}}^{\frac{h(z)}{2}} \frac{\pi E\rho^2}{(1+v)(1-2v)} d\rho,\ f_9 = 2v\phi_r \frac{\partial \phi_z}{\partial z},\ B_1(z) = \pi \int_{-\frac{h(z)}{2}}^{\frac{h(z)}{2}} \frac{\alpha(R+\rho)ET}{1-2v} d\rho,\ g_1 = \phi_\rho + \frac{\partial u}{\partial z},$$

$$B_2(z) = \pi \int_{-\frac{h(z)}{2}}^{\frac{h(z)}{2}} \rho \frac{\alpha(R+\rho)ET}{1-2v} d\rho,\ g_2 = \frac{\partial \phi_z}{\partial z},\ B_3(z) = \pi \int_{-\frac{h(z)}{2}}^{\frac{h(z)}{2}} \frac{\alpha ET}{1-2v} d\rho,\ g_3 = w, B_4(z) = \pi \int_{-\frac{h(z)}{2}}^{\frac{h(z)}{2}} \rho \frac{\alpha ET}{1-2v} d\rho,\ g_4 = \phi_r$$

2.1. Calculation of external works

Energy of internal and external pressure is equal to multiplying of pressure in the radial deformation of the inner and the other surface of the cylinder, respectively. Inner pressure applies in the same direction of the positive deformation; conversely, outer pressure applies in the negative direction of the deformation. Eq. (11) indicates the external work W due to internal and external pressure. Fig. 1 shows the schematic figure of a cylindrical pressure vessel

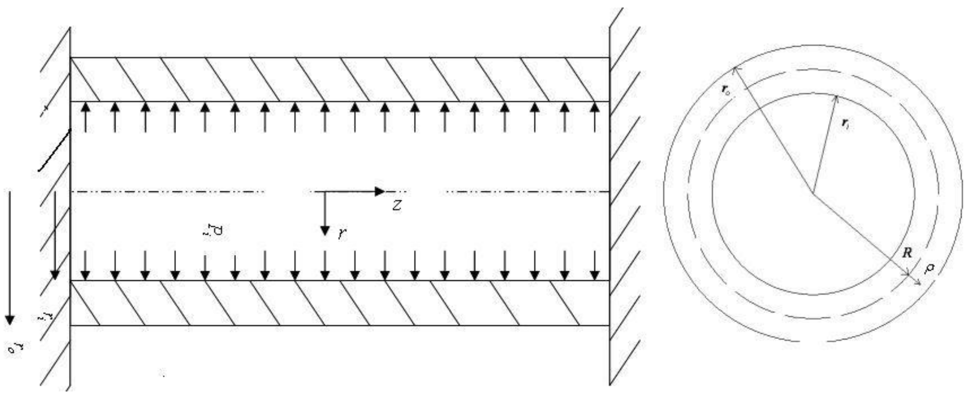

Fig. 1 Tthe schematic figure of a cylinder with fixed edges

$$
\left.
\begin{aligned}
&W=\int_0^l [C_1 w + C_2\phi_r]dz=\int_0^l W_z dz\\
&C_1=2\pi\left(P_i\left(R-\frac{h}{2}\right)-P_0\left(R+\frac{h}{2}\right)\right)\\
&C_2=2\pi\frac{h}{2}\left(-P_i\left(R-\frac{h}{2}\right)-P_0\left(R+\frac{h}{2}\right)\right)
\end{aligned}
\right\}
\tag{11}
$$

In the present paper, only internal pressure is considered. Therefore, we'll have

$$
C_1=2\pi P_i\left(R-\frac{h}{2}\right),\quad C_2=-2\pi\frac{h}{2}P_i\left(R-\frac{h}{2}\right)
$$

2.2. Variation of the energy equation

Total energy of the system must be obtained by subtraction of Eq. (11) from Eq. (9) as follows

$$
U=\int_0^l (U_S-U_T)dz-\int_0^l W_z dz=\int_0^l F(u,w,\phi_z,\phi_r,z)dz \tag{12}
$$

As mentioned above, Eq. (12) includes four variables. Governing differential equation of the system may be obtained by minimization of the energy equation with respect to four assumed variables. By using Euler equation, variation of Eq. (12) can be expressed as follows

$$
\begin{cases}
1)\ \dfrac{\partial F}{\partial u}-\dfrac{\partial}{\partial z}\left(\dfrac{\partial F}{\partial\left(\dfrac{\partial u}{\partial z}\right)}\right)=0\\
2)\ \dfrac{\partial F}{\partial \phi_z}-\dfrac{\partial}{\partial z}\left(\dfrac{\partial F}{\partial\left(\dfrac{\partial \phi_z}{\partial z}\right)}\right)=0\\
3)\ \dfrac{\partial F}{\partial w}-\dfrac{\partial}{\partial z}\left(\dfrac{\partial F}{\partial\left(\dfrac{\partial w}{\partial z}\right)}\right)=0\\
4)\ \dfrac{\partial F}{\partial \phi_r}-\dfrac{\partial}{\partial z}\left(\dfrac{\partial F}{\partial\left(\dfrac{\partial \phi_r}{\partial z}\right)}\right)=0
\end{cases}
\tag{13}
$$

where functional $F(u,w,\phi_z,\phi_r,z)$ is introduced using the Eq. (12). Equilibrium Eq. (13), which are obtained from Eq. (12), can be represented in terms of resultant of moments and forces. This procedure diminishes the long mathematical equations. Resultant of moments M_i and forces N_i in terms of stress components are [17]

$$
\left.
\begin{aligned}
&N_z=\int_{-\frac{h(z)}{2}}^{\frac{h(z)}{2}}\sigma_z\left(1+\frac{\rho}{R}\right)d\rho,\ N_\theta=\int_{-\frac{h(z)}{2}}^{\frac{h(z)}{2}}\sigma_\theta d\rho,\\
&N_r=\int_{-\frac{h(z)}{2}}^{\frac{h(z)}{2}}\sigma_r\left(1+\frac{\rho}{R}\right)d\rho,\ M_z=\int_{-\frac{h(z)}{2}}^{\frac{h(z)}{2}}\sigma_z\left(1+\frac{\rho}{R}\right)\rho d\rho,\\
&M_\theta=\int_{-\frac{h(z)}{2}}^{\frac{h(z)}{2}}\sigma_\theta\rho d\rho,\ M_{rz}=\int_{-\frac{h(z)}{2}}^{\frac{h(z)}{2}}\tau_{rz}\left(1+\frac{\rho}{R}\right)\rho d\rho\\
&Q_r=\int_{-\frac{h(z)}{2}}^{\frac{h(z)}{2}}\tau_{rz}\left(1+\frac{\rho}{R}\right)d\rho
\end{aligned}
\right\}
\tag{14}
$$

Therefore, the main governing relations of the thermo-elastic behavior of a functionally graded cylinder can be expressed as follows [17]

$$
\begin{cases}
\dfrac{\partial N_z}{\partial z}=0\\
N_\theta-\dfrac{\partial}{\partial z}[RQ_r]+\dfrac{1}{2\pi}B_3(z)=P_i\left(R-\dfrac{h}{2}\right)\\
Q_r-\dfrac{1}{R}\dfrac{\partial}{\partial z}\left[RM_z+\dfrac{B_2(z)}{2\pi}\right]=0\\
\left[RN_r+\dfrac{B_1(z)}{2\pi}\right]+\left[M_\theta+\dfrac{B_4(z)}{2\pi}\right]-\dfrac{\partial}{\partial z}[RM_{rz}]=\\
=-\dfrac{h}{2}P_i\left(R-\dfrac{h}{2}\right)
\end{cases}
\tag{15}
$$

where $B_i(z)$ are the functions of the thermal conditions. Eqs. (15) is the second order system of differential equation with four variables

$$
\left.
\begin{aligned}
&[G_1]\frac{d^2}{dz^2}\{X\}+[G_2]\frac{d}{dz}\{X\}+[G_3]\{X\}=\{F\}\\
&\{X\}=\left[u(z)\ \ \phi_z(z)\ \ w(z)\ \ \phi_r(z)\right]^T
\end{aligned}
\right\}
\tag{16}
$$

Eq. (16) shows the matrix presentation of Eqs. (15). With applying the appropriate matrix operations to the Eq. (16), G_1,G_2,G_3 and force vector $F(z)$ may be obtained using Eqs. (17). G_1,G_3 are symmetric matrices and G_2 is an anti symmetric matrix and can be obtained as follows

$$
\left.
\begin{aligned}
&G_1)_{11}=(1-v)A_1, G_1)_{12}=(1-v)A_2, G_1)_{22}=(1-v)A_3,\\
&G_1)_{33}=\frac{1-2v}{2}A_1, G_1)_{34}=\frac{1-2v}{2}A_2, G_1)_{44}=\frac{(1-2v)}{2}A_3\\
&G_2)_{13}=-G_2)_{31}=vA_4, G_2)_{14}=-G_2)_{41}=v(A_6+A_1),\\
&G_2)_{23}=-G_2)_{32}=-\frac{1-2v}{2}A_1+vA_6,\\
&G_2)_{24}=-G_2)_{42}=-\frac{1-2v}{2}A_2+v(A_2+A_9)\\
&G_3)_{22}=-\frac{1-2v}{2}A_1, G_3)_{34}=-(1-v)A_7-vA_4\\
&G_3)_{44}=-(1-v)(A_8+A_1)-2vA_6, G_3)_{33}=-(1-v)A_5
\end{aligned}
\right\}
\tag{17}
$$

Eqs. (16) and (17) are the complete governing equations of a FG cylinder that are derived yet. In the following section, we must solve the governing differential Eq.16 for general boundary conditions.

3. Two dimensional solution of a FG cylinder

The important objective of this study is the investigation on the end effect of cylinder on the response of the cylinder. For attaining to this purpose, it is inevitable to obtain the homogenous solution of Eq. (16). Homogenous solution of this problem includes eight constants of integration. These constants can be obtained by consideration of the natural boundary condition of two ends of the cylinder. Homogenous solution of Eq. (16) in the general form is (subscript *h* shows that this solution is a homogenous solution):

$$X_h{}^j = \sum_{i=1}^{8} c_i v^i{}_j e^{m_i z} \tag{18}$$

Eq. (18) in the extended form is

$$\begin{bmatrix} u \\ w \\ \phi_z \\ \phi_r \end{bmatrix}_h = \begin{bmatrix} v^1{}_1 & v^2{}_1 & v^3{}_1 & v^4{}_1 & v^5{}_1 & v^6{}_1 & v^7{}_1 & v^8{}_1 \\ v^1{}_2 & v^2{}_2 & v^3{}_2 & v^4{}_2 & v^5{}_2 & v^6{}_2 & v^7{}_2 & v^8{}_2 \\ v^1{}_3 & v^2{}_3 & v^3{}_3 & v^4{}_3 & v^5{}_3 & v^6{}_3 & v^7{}_3 & v^8{}_3 \\ v^1{}_4 & v^2{}_4 & v^3{}_4 & v^4{}_4 & v^5{}_4 & v^6{}_4 & v^7{}_4 & v^8{}_4 \end{bmatrix} \begin{bmatrix} c_1 e^{m_1 z} \\ c_2 e^{m_2 z} \\ c_3 e^{m_3 z} \\ c_4 e^{m_4 z} \\ c_5 e^{m_5 z} \\ c_6 e^{m_6 z} \\ c_7 e^{m_7 z} \\ c_8 e^{m_8 z} \end{bmatrix} \tag{19}$$

where m_i is the eigen value of the problem that is obtained from the characteristic Eq. (20) as follows

$$[G_1 m^2 + G_2 m + G_3]\{v\} = 0 \tag{20}$$

Due to the nonzero vector *v*, characteristic equation of this problem can be obtained by determinant of the matrix of $[G_1 m^2 + G_2 m + G_3]$

$$det[G_1 m^2 + G_2 m + G_3] = 0 \tag{21}$$

Obtained characteristic Eq. (21) is an eight's order equation. With solving the characteristic Eq. (21), eight roots of Eq. (21) can be obtained. With substitution of every root m_i in Eq. (20), corresponding eigen vector v_i can be obtained. $v^i{}_k\ (k = 1,2,3,4)$ constitutes the *i* th column of Eq. (19) for root m_i. Particular solution of Eq. (16) is:

$$[G_3]\{X\}_p = \{F\} \rightarrow \{X\}_p = [G_3]^{-1}\{F\} \tag{22}$$

Therefore, we'll have the final solution of the problem as follows

$$\{X\} = \{X\}_h + \{X\}_p \tag{23}$$

Two dimensional solution of the cylinder can be completed with imposing the appropriate boundary conditions on Eq. (23). For a cylinder with clamped-clamped or two simply supported ends, the boundary conditions can be presented as follows, respectively

$$\left.\begin{array}{l} \text{Clamped – clamped} \\ u = w = \sigma_z = \sigma_\theta = 0 \ \text{ at } z = L/2 \\ \dfrac{\partial u}{\partial z} = \dfrac{\partial w}{\partial z} = \dfrac{\partial \psi_z}{\partial z} = \dfrac{\partial \psi_r}{\partial z} = 0 \ \text{ at } z = 0 \\ \text{Simply supporte} \\ u = w = \psi_z = \psi_r = 0 \ \text{ at } z = L/2 \\ \dfrac{\partial u}{\partial z} = \dfrac{\partial w}{\partial z} = \dfrac{\partial \psi_z}{\partial z} = \dfrac{\partial \psi_r}{\partial z} = 0 \ \text{ at } z = 0 \end{array}\right\} \tag{24}$$

For other boundary conditions, the presented method has capability to solve problem, exactly.

Example: solution of a clamped-clamped cylinder

Two end of cylinder are assumed to be fixed and clamped. Therefore, deflections and rotations vanish at the two ends of the cylinder. Due to imposing the similar boundary condition on the two ends of cylinder, the slope of the deflections and rotations vanishes at the middle of the cylinder.

4. Numerical results, comparison and discussion

In the present section, results of thermo-elastic analysis can be investigated numerically. It is supposed that the modulus of elasticity *E* is graded in the radial direction only, *E(r)*. Before numerical evaluation, non-homogenous modulus of elasticity must be defined as a power function of the radial coordinate as follows

$$E = E_i(\bar{r})^n = E_i\left(\frac{r}{r_i}\right)^n \xrightarrow{r=R+\rho}$$

$$E = E_i(\bar{r})^n = E_i\left(\frac{R+\rho}{r_i}\right)^n = \frac{E_i}{r^n{}_i}(R+\rho)^n$$

The numerical values are considered as follows

$$E_i = 2\times10^{11}\,\text{Pa},\ \alpha = 5\times10^{-6}\ {}^{1}/{}_{^\circ\text{C}},\ \nu = 0.3,$$

$$r_i = 0.04\ \text{m},\ r_0 = 0.06\ \text{m},\ L = 1.6\ \text{m},\ R = 0.05\ \text{m}$$

4.1. Studying of the results in the presence of temperature only

4.1.1. Axial and radial displacement

In the present section, it is supposed that only temperature rising (150°C) is applied. Fig. 2 shows the axial distribution of the axial displacement along the assumed axial direction as depicted in Fig. 1. The effect of four values of nonhomogenous index (*n*) is investigated in the Fig. 2. Fig. 2 shows that the value of displacement changes abruptly at the near of the end of the cylinder. This changes lead to the major strains and stresses. The effect of this alteration on the local stresses may be studied in the following section. As a far from distance of the end of the cylinder $2x/L \leq 0.875$, displacement of the cylinder tend to an asymptotic value. This figure shows that the absolute value of the axial displacement decreases with increasing of the nonhomogenous index *n*.

Fig. 3 shows the axial distribution of the radial displacement for different values of nonhomogenous index *n*. This figure shows that the value of the radial displacement increases with increasing of the nonhomogenous index *n*.

4.1.2. Shear and axial stresses

Figs. 4 and 5 show the axial distribution of the shear and axial stresses, respectively. As depicted in the Fig. 4, the shear stress is zero at the whole of the cylinder except at the end of that. The shear stress at the end of cylinder for $n = 1$ is about 270 MPa. This large value of stress tends to local stress concentration at the end of cylinder. Composition of this stress with the other component of stress, tend to the local yielding at the end of cylinder. Fig. 4 shows that the assumption of zero shear stress is valid for the whole of the cylinder except the end of the cylinder. Fig. 5 shows the axial distribution of the axial stress. As depicted in this figure, the magnitude of the axial stress at the end of cylinder is about 2 times of stress at the middle of the cylinder (stress concentration factor = 2).

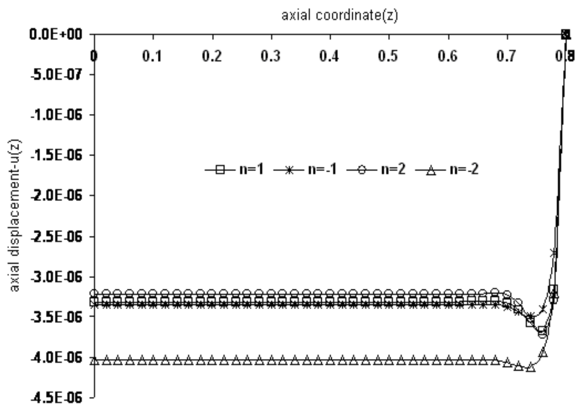

Fig. 2 The axial distribution of the axial displacement of the midsurface of cylinder ($z = 0$) in the presence of temperature only

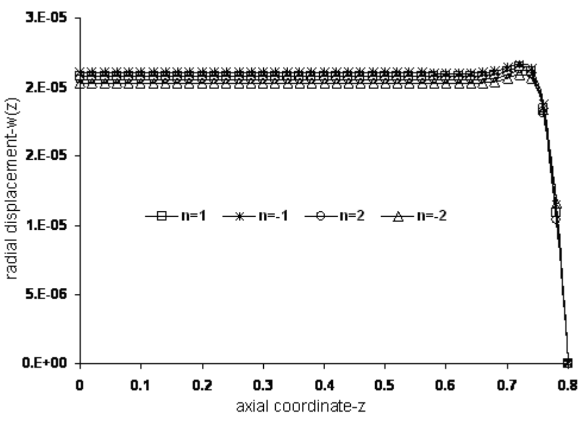

Fig. 3 The axial distribution of the radial displacement of the midsurface of cylinder ($z = 0$) in the presence of temperature only

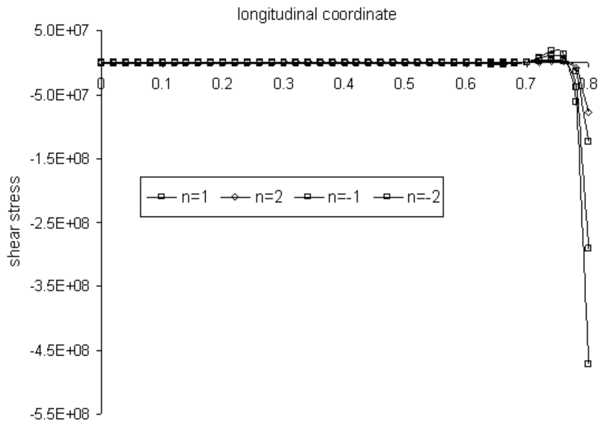

Fig. 4 The axial distribution of shear stress at the outer layer of cylinder (under temperature only)

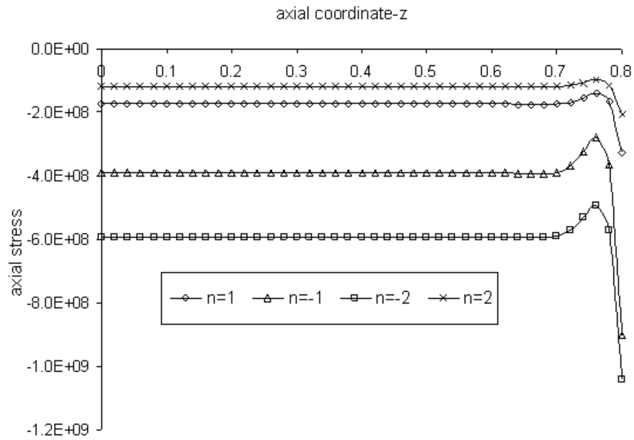

Fig. 5 The axial distribution of axial stress at the outer layer of cylinder (under temperature only)

4.2. Results for simultaneously presence of the temperature and inner pressure

4.2.1. Axial and radial displacement

In this section, it is supposed that an inner pressure 80 MPa applies on the cylinder with a temperature rising 150°C. Fig. 6 shows the axial distribution of

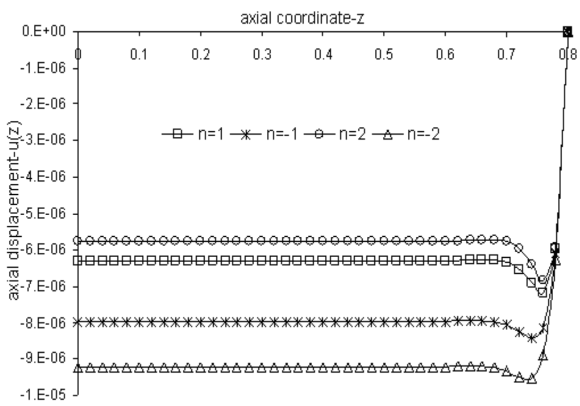

Fig. 6 The axial distribution of the axial displacement of the midsurface of cylinder ($z = 0$) in the presence of temperature and pressure

the axial displacement of the midsurface of the cylinder (z = 0) in the simultaneously presence of the temperature and inner pressure. This figure indicates that the absolute value of the axial displacement increases with decreasing of the non-homogenous index n. These results are in accordance with the literature [7].

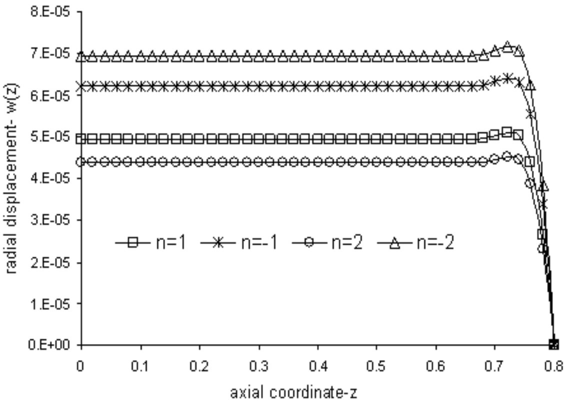

Fig.7 The axial distribution of the radial displacement of the midsurface of cylinder(z = 0) in the presence of temperature and pressure

Fig. 7 shows the axial distribution of the radial displacement of the midsurface of the cylinder (z = 0). This figure shows that the absolute value of the axial displacement increases with decreasing of the non-homogenous index n.

4.2.2. Shear and axial stresses

Figs. 8 and 9 show the axial distribution of the shear and axial stresses, respectively. As depicted in the Fig. 8, the shear stress is zero at the whole location of the cylinder except at the end of cylinder. Fig. 9 shows the axial distribution of the axial stress. As depicted in this figure, the magnitude of the axial stress at the end of cylinder is about 2 times of stress at the middle of the cylinder.

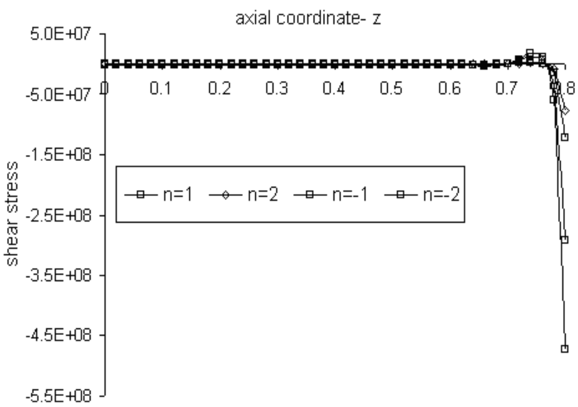

Fig. 8 The longitudinal distribution of shear stress at the outer layer of cylinder (under pressure and temperature)

4.3. Two dimensional distribution of displacements

Figs. 10 and 11 show the two dimensional distribution of axial and radial displacement of a FG cylinder under temperature rising only.

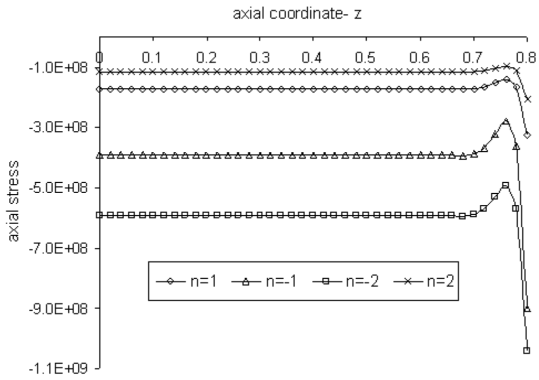

Fig. 9 The longitudinal distribution of axial stress at the outer layer of cylinder (under temperature and pressure)

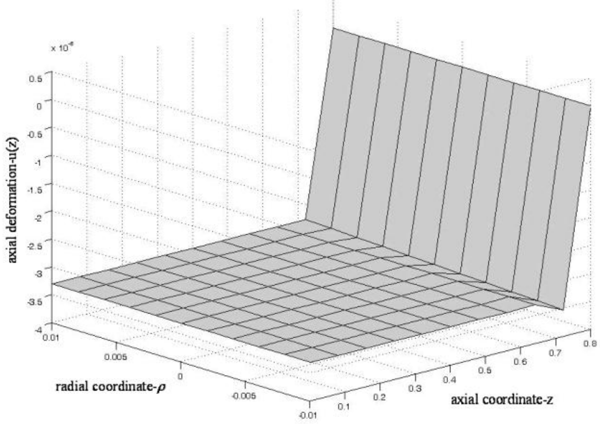

Fig. 10 The two dimensional distribution of the axial deformation under temperature rising only

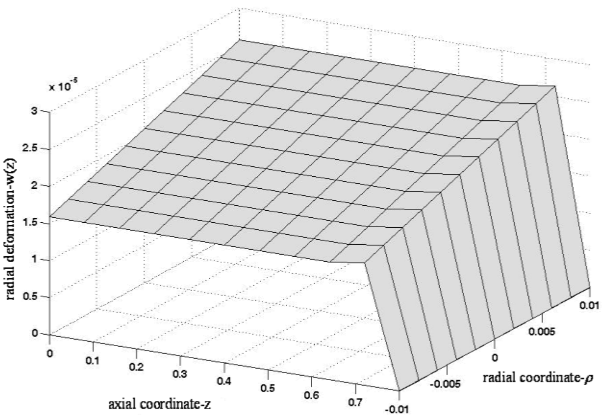

Fig. 11 The plane distribution of the radial deformation under temperature rising only

4.4. Comparison of the present results with finite element method

The results of this paper are obtained analytically by considering the homogenous and particular solution of the Eq. (16) and imposing the appropriate boundary condition. The obtained results can be compared with the numerical results obtained using the finite element method. Shown in Fig. 12 is comparison between the results using the first order shear deformation theory and finite element method. It is observed that the maximum difference between the results is about 8%. This insignificant difference can justifies the present results, carefully.

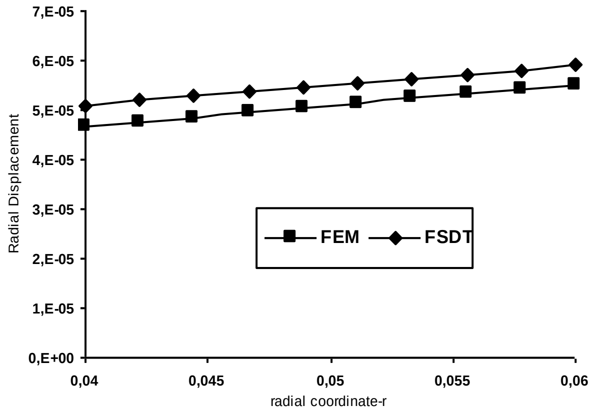

Fig. 12 Comparing of present results with the numerical results (FEM)

5. Conclusions

The extracted conclusions are classified as follows:

1. Comprehensive thermoelastic analysis of a thick walled FG cylinder with different boundary conditions under inner pressure is investigated in the present paper based on the FSDT. In the previous paper, it is not recognized the effect of arbitrary end supports and the effect of the thermal strains on this theory [13-15]. For the first time, exact two-dimensional (radial and axial) analysis of a FG cylinder is investigated and the obtained results are compared with the numerical results (FEM).

2. In the presence of temperature rising only, achieved results show that the absolute value of axial displacement of the cylinder decreases with increasing of the nonhomogenous index n. The radial displacement increases with increasing of the nonhomogenous index n.

3. Because of abrupt changing of displacement at the near of two ends of the cylinder, the value of stresses at the end of the cylinder are very greater than the stresses at the middle of the cylinder. These stresses tend to local yielding at the end of cylinder. The present results can be applied for calculation of the stress concentration factor due to end supports.

4. Comparison between the present results (two-dimensional cylinder with the clamped ends) with the numerical results (FEM) indicates that the maximum difference between them is not significant. Therefore, the present method has many advantageous to justify application of that in thermo elastic analysis of a thick walled structure. For example, the thermal and mechanical analysis of a functionally graded truncated conical shell can be studied using the presented method in this paper. The stress and displacement analyses of this problem are not considered in the previous studies [18].

References

1. **Khoshgoftar, M.J.; G. Arani, A.; Arefi, M.** 2009. Thermoelastic analysis of a thick walled cylinder made of functionally graded piezoelectric material, Smart. Mater. Struct. 18: 115007.
2. **Timoshenko, S.P.** 1976. Strength of Materials: Part II (Advanced Theory and Problems), 3 rd edition, Van Nostrand Reinhold Co. New York.
3. **Naghdi, P.M.; Cooper, R.M.** 1956. Propagation of elastic waves in cylindrical shells including the effects of transverse shear and rotary inertia, J. Acoustical Sc. America. 28(1): 56-63.
4. **Mirsky, I.; Hermann, G.** 1958. Axially motions of thick cylindrical shells, J. Appl. Mech. 25: 97-102.
5. **Yamanouchi, M.; Koizumi, M.; Shiota, I.** 1990. Proceedings of the First International Symposium on Functionally Gradient Materials, Sendai, Japan.
6. **Tutuncu, N.; Ozturk, M.** 2001. Exact solution for stresses in functionally graded pressure vessels, Compos. Part B. Eng. 32: 683-686.
7. **Jabbari, M.; Sohrabpour, S.; Eslami, M.R.** 2002. Mechanical and thermal stresses in a functionally graded hollow cylinder due to radially symmetric loads, Int. J. Pres. Ves. Pip. 79: 493-497.
8. **Wu, L.; Zhiqing, J.; Jun L.** 2005. Thermoelastic stability of functionally graded cylindrical shells, Compos. Struct. 70: 60-68.
9. **Shao, Z.S.** 2005. Mechanical and thermal stresses of a functionally graded circular hollow cylinder with finite length, Int. J. Pres. Ves. Pip. 82: 155-163.
10. **Eslami, M.R.; Babaei, M.H.; Poultangari, R.** 2005. Thermal and mechanical stresses in a functionally graded thick sphere, Int. J. Pres. Ves. Pip. 82: 522-527.
11. **Bahtui, A.; Eslami, M.R.** 2007. Coupled thermoelasticity of functionally graded cylindrical shells, Mech. Res. Commun. 34: 1-18.
12. **S. Khabbaz, R.; D. Manshadi, B.; Abedian, A.** 2009. Non-linear analysis of FGM plates under pressure loads using the higher-order shear deformation theories, Compos. Struct., 89: 333-344.
13. **Jabbari, M.; Bahtui, A.; Eslami, M.R.** 2009. Axisymmetric mechanical and thermal stresses in thick short length FGM cylinders, Int. J. Pres. Ves. Pip. 86(5): 296-306.
14. **Ghannad, K.M.; Rahimi, G.H.; E. Khadem, S.** 2008. General Plane Elasticity Solution of Axisymmetric Functionally Graded Thick Cylinderical Shells, Modares Technical and Engineering [in Persian].
15. **Ghannad, K.M.; Rahimi, G.H.; E. Khadem, S.** 2008. General Shear Deformation Solution of Axisymmetric Functionally Graded Thick Cylinderical Shells, Modares Technical and Engineering [In persian].
16. **Nejad, Z.M.; Rahimi, G.H.; Ghannad. K,M.** 2009. Set of field equations for thick shell of revolution made of functionally graded materials in curvilinear coordinate system, Mechanika 3(77): 18-26.
17. **Ghannad, M.Z.; Nejad, M.; Rahimi, G.H.** 2009. Elastic solution of axisymmetric thick truncated conical shells based on first-order shear deformation theory, Mechanika 5(79): 13-20.
18. **Naj R.S.; Boroujerdy, M.; Eslami, M.R.** 2008. Thermal and mechanical instability of functionally graded truncated conical shells, Thin. Wall. Struct. 46: 65-78.

M. Arefi, G.H. Rahimi

IŠSAMI SKIRTINGOMIS RIBINĖMIS SĄLYGOMIS KOKYBIŠKAI VEIKIANČIO VIDINIU SLĖGIU APKRAUTO CILINDRO ŠILUMINĖ TAMPRIOJI ANALIZĖ, PAREMTA PIRMOS EILĖS ŠLYTIES DEFORMACIJOS TEORIJA

R e z i u m ė

Šiame darbe, remiantis pirmos eilės šlyties deformacijos teorija, atliekama skirtingomis ribinėmis sąlygomis kokybiškai veikiančio vidiniu slėgiu apkrauto cilindro šiluminė tamprioji analizė. Straipsnyje siūlomas sprendimas leidžia apskaičiuoti cilindro konstrukciją esant nustatytoms ribinėms sąlygoms. Atliekant pradinį tyrimą buvo pasiūlyta problemą spręsti esant paprastoms ribinėms sąlygoms (kai cilindras elementariai palaikomas). Šiame straipsnyje tiriamas ašinių poslinkių ir įtempių pasiskirstymas esant skirtingam nehomogeniškumo laipsniui. Tyrimas rodo, kad cilindro įtvirtinimas turi didelę įtaką mechaninių komponentų pasiskirstymui ir jo negalima neįvertinti. Kartu nagrinėta temperatūros ir slėgio įtaka cilindro deformacijoms ir įtempiams. Įtempių koncentracijos koeficiento skaičiavimas, atsižvelgiant į įtvirtinimo efektą, yra kitas šio straipsnio rezultatas. Pateikti rezultatai yra patvirtinti lyginant su ankstesniais rezultatais, gautais remiantis plokštumos tamprumo teorija.

M. Arefi, G.H. Rahimi

COMPREHENSIVE THERMOELASTIC ANALYSIS OF A FUNCTIONALLY GRADED CYLINDER WITH DIFFERENT BOUNDARY CONDITIONS UNDER INTERNAL PRESSURE USING FIRST ORDER SHEAR DEFORMATION THEORY

S u m m a r y

This paper deals with the thermo elastic analysis of a FG cylinder with different boundary conditions under internal pressure using the first order shear deformation theory. This proposed solution has the ability to solve the cylinder structure with arbitrary boundary conditions. The previous studies have been proposed for the problem with simple boundary conditions (simply supported cylinder). This paper investigates the axial distribution of the displacement and stress for different values of non-homogenous index. This investigation indicates that a support has important influence on the distribution of mechanical components rather than a cylinder with ignoring the effect of support. Simultaneously effect of the temperature and pressure are studied on the deformation and stress of cylinder. Calculation of the stress concentration factor due to end effects is another result of the present paper. The presented results are validated by comparison with previous results that have been evaluated using the plane elasticity theory.

Keywords: comprehensive thermoelastic analysis, first order shear deformation theory.

Received February 25, 2011
Accepted February 09, 2012